

# Geometric optimisation of a micromachine with a spiral tail immersed in viscous medium

S. Nasser, N. Phan-Thien

267

**Abstract** A model of micromachine with a spiral tail moving in a highly viscous fluid has been simulated using the Boundary Element Method. The trajectory of this micromachine is a straight line and it swims with a velocity close to that of a microorganism with a helical tail. An optimisation process has been carried out in order to find the optimal parameters to obtain the highest translational velocity. The optimum capsule-shaped head of this micromachine has an aspect ratio of about 0.5; the length of the tail is about 8 times the radius of the head, about 4.2 times of its width, and consists of 1.5 wavelengths. The dimensional proportions obtained here are in excellent agreement with previous studies on the motion of microorganisms with helical tails.

## Nomenclature

$L_t$	Length of the tail
$b$	Width of the tail
$L_h$	Length of the head
$a$	Radius of the head
$\nu$	Kinematic viscosity
$\lambda$	Tail wavelength
$P$	Dissipated power
$p$	Hydrostatic pressure
$U$	Propulsion velocity of the head or $U_h$
$\Omega$	Angular velocity of the head or $\Omega_h$
$\omega$	Angular velocity of the tail relative to the head
$N_w$	Wave number
$l$	Intermediate length of the head
$c$	Wave phase velocity
$K$	Wave parameter

## 1

### Introduction

This paper is concerned with some hydrodynamic aspects of the motion of a micromachine in a viscous fluid. The

mechanical model of this micromachine adopted for the present study consists of a capsule-shaped head and a rigid spiral shape tail which rotates relative to the head and induces a propulsive force and associated torque on the head. As a result, the whole machine acquires a swimming speed  $U$  and rigid-body rotation  $\Omega$ . Finding the rigid body motion of the machine, and the optimal geometry for the head and the tail to maximise the swimming speed is the purpose of this paper.

The Reynolds number based on the body length or any other characteristic linear dimension of the body, here  $L_t$ , and its mean forward velocity  $U$  is supposed to be very small, *i.e.*,  $Re = UL_t/\nu \ll 1$ , where  $\nu$  is the kinematic viscosity of the fluid. Hence the predominant forces acting on the micromachine are viscous forces; inertia and body forces can be neglected. In this case the relevant governing equations are the Stokes equations. As an example, a micromotor of a linear dimension of 100  $\mu\text{m}$ , moving at a speed of 100 RPM in air has a Reynolds number of 0.007.

Extensive works have been done on analysing the motion of microorganism of different types moving in viscous fluid. This field of study is appropriately referred to as *Flagellar Hydrodynamic*, which has been thoroughly reviewed by Lighthill (1976). Although initial mathematical models for flagellar motions were developed by Taylor (1951, 1952), models for large-amplitude motions of flagella on a microorganism were first proposed by Hancock (1953). However, Hancock's method did not account for the head (cell body) which is present in most flagellar microorganisms. Later, Gray and Hancock (1955) developed a technique that accounted for the cell-body drag. They adopted a set of resistance coefficients which were derived from Hancock's previous work with planar waves and applied the *resistive-force theory* to analyse the motion of a flagellar microorganism that swims by passing sinusoidal planar waves down its flagellum. This theory was also extended to cover the helical-wave case. However, Chwang and Wu (1971) noted that the propagation of the helical-wave along the flagellum induces a torque on the microorganism. Thus, the body also rotates with an angular velocity in response to this propulsive torque. They derived expressions for the swimming and angular velocities as well as power requirements which were used to determine the optimum proportions of a given microorganism. Also, Keller and Rubinow (1976) showed that the swimming trajectory for a microorganism with a helically beating flagellum is itself helical. They derived analytical expressions for the radius, period and the pitch angle of the trajectory in terms of the instantaneous swimming

Communicated by S. N. Atluri, 17 February 1997

S. Nasser, N. Phan-Thien  
Department of Mechanical and Mechatronics Engineering,  
The University of Sydney, N.S.W. 2006, Australia  
E-mail: nhan@mech.eng.usud.edu.au

Correspondence to: N. Phan-Thien

This research is supported by the Australian Research Council. The use of the computational facility of the Sydney Distributed Computing (SyDCom) Laboratory is acknowledged.

velocity and angular velocity. Phan-Thien et al. (1987), analysed the swimming of a flagellar microorganism by the propagation of helical waves along its flagellum using the Boundary Element Method. In their work, optimum helical wave parameters as well as the optimal dimensional geometry parameters were derived to obtain the minimum power dissipation.

From the results of our previous research (Nasseri and Phan-Thien 1996), on designing a special type of micromachine consisting of a “head” and a “rigid tail” immersed in a viscous medium, it was demonstrated that no averaged propulsive force would be produced. Therefore a more complex shape for the tail, of the types commonly seen in microorganisms, was suggested. The model of the micromachine introduced here is somewhat different from the microorganism with helical tail, but it has about the same swimming efficiency and it is easier to manufacture than a sperm-like micromachine.

Recently “surface micromachining” techniques have received considerable attention (see French 1996). In this case the mechanical structures are fabricated in thin films deposited on a silicon water surface. This development has yielded structures considerably smaller than those fabricated in “bulk micromachining”. By using the method of surface micromachining, a flat rectangle sheet, which is in fact a polysilicon layer, is deposited on the surface of intermediate layer of silicon dioxide which is deposited itself on a substrate of silicon. Finally, the entire substrate is placed in an etch which dissolves away the oxide and the desired rectangle would be released. The aspect ratio of these structures are typically quite large, being several hundred microns in the lateral dimension and only 1–2 microns in the vertical dimension. That is the reason we consider zero thickness for the tail in this note; however, the technique can accommodate a finite thickness of the tail without any modification to the software. After manufacturing a flat rectangular sheet, then this sheet can be twisted about the principal centreline and formed a spiral tail for our micromachine. The head contains a micromotor which provides a rotation of the tail relative to the head. Different geometry for the head and the tail was adopted to maximise the swimming velocity for this micromachine.

## 2

### Boundary-integral formulation

The boundary-integral formulation for linear elastic problems (including Stokes flow problems in three dimensions) is well known and has been documented elsewhere, e.g., Banerjee and Butterfield (1981) and Brebbia et al. (1984). The advantage of the method is the automatic treatment of flow conditions at infinity; only the boundary of the body, or bodies, requires discretization, decreasing enormously the number of unknowns in the problem.

Here, this method is briefly reviewed as applied to Stokes flow problems in which the governing equations are

$$\mu \nabla^2 \mathbf{u} = \nabla p, \quad \nabla \cdot \mathbf{u} = 0, \quad \mathbf{x} \in D, \quad (1)$$

where  $\mathbf{u}$  is the velocity vector,  $p$  is the hydrostatic pressure which arises owing to the incompressibility constraint,  $\mu$  is the constant viscosity of the fluid and  $D$  is the flow domain. These equations are applicable to the motion of fluid around

the micromachine as the Reynolds number based on the length scale of the machine is extremely small. The velocity field can be expressed in terms of surface integrals involving the boundary velocity and traction fields. The technique is standard and the reader is referred to, for example, Banerjee and Butterfield (1981) and Brebbia et al. (1984).

In the constant BEM, the body is discretised into  $N$  triangular boundary elements, on which both velocity and traction fields remain constant, and the set of boundary integral equations leads to

$$c_{ij}(\mathbf{x}) u_j(\mathbf{x}) = \sum_{n=1}^N \left\{ u_j^{(n)} \int_{S_n} u_{ij}^*(\mathbf{x}, \mathbf{X}) dS(\mathbf{X}) - t_j^{(n)} \int_{S_n} t_{ij}^*(\mathbf{x}, \mathbf{X}) dS(\mathbf{X}) \right\}, \quad (2)$$

where  $\mathbf{u}^{(n)}$  is the velocity and  $\mathbf{t}^{(n)}$  is the traction on element  $n$ ,  $\mathbf{x}$  is the field point which belongs to element  $p$  and  $\mathbf{X}$  belongs to element  $n$ ,  $u_{ij}^*(\mathbf{x}, \mathbf{X})$  and  $t_{ij}^*(\mathbf{x}, \mathbf{X})$  are known kernels (the Stokeslet and the adjoint of the traction of the Stokeslet). In addition, for a smooth surface,

$$c_{ij}(\mathbf{x}) = \begin{cases} \delta_{ij}, & \mathbf{x} \text{ in the interior of } D, \\ \frac{1}{2} \delta_{ij}, & \mathbf{x} \text{ on the boundary of } D, \\ 0, & \mathbf{x} \text{ in the exterior of } D. \end{cases}$$

This leads to a linear algebraic equation (see Phan-Thien et al., 1987 or Nasseri and Phan-Thien, 1996)

$$\mathbf{H}\mathbf{u} = \mathbf{G}\mathbf{t}, \quad (3)$$

where,  $\mathbf{H}$  and  $\mathbf{G}$  are known  $3N \times 3N$  matrices depending only on the geometry of the boundary, and not on the prescribed boundary conditions.

For a micromachine whose tail rotates relative to the head with a known angular velocity  $\omega$ , together with the fact that the machine translates as a rigid body give rise to the kinematic constraints

$$\mathbf{\Omega}_t = \mathbf{\Omega}_h + \omega, \quad \mathbf{U}_t = \mathbf{U}_h, \quad (4)$$

where  $t$  denotes a tail quantity and  $h$ , a head quantity. The angular velocity  $\omega$ , which is treated as an independent parameter, has a direction along tail's centreline and a fixed magnitude  $\omega$ . In the present calculations, both  $\omega$  and fluid viscosity,  $\mu$  are normalized to 1; thus time is normalized with respect to  $\omega^{-1}$ , and stresses are normalized with respect to  $\mu\omega^{-1}$ .

For a body propelling itself at a constant mean velocity in a viscous fluid, both the resultant force and torque acted on the body by the fluid must vanish. This yields six equations relating twelve flow quantities, the translational propulsion velocity,  $\mathbf{U}$ , the induced angular velocity  $\mathbf{\Omega}$  of the body, the resultant thrust  $\mathbf{F}$  and the resultant torque  $\mathbf{M}$  experienced by the machine. The conditions of force-free and torque-free can then be imposed to obtain the rigid body motion of the micromachine from which the scalar forward speed  $U$  and the angular velocity  $\Omega$  about the mean direction of motion (here the principal axis of the spiral,  $z$ ) of a micromachine can be determined.

The instantaneous power dissipated  $P$  for this micromachine is calculated using (integral of the scalar product of the traction and the velocity fields):

$$P = \sum_{n=1}^N S_n \mathbf{t}^{(n)} \cdot \mathbf{u}^{(n)} ,$$

where  $\mathbf{u}^{(n)}$  is regarded as

$$\mathbf{u}^{(n)} = \mathbf{U} + (\boldsymbol{\Omega} + k\boldsymbol{\omega}) \times \mathbf{x}^{(n)} .$$

Here  $\mathbf{U}$  is the absolute velocity of an arbitrary head/tail joining point of the head and the tail,  $\boldsymbol{\Omega}$  is the angular velocity of the head about this point,  $\mathbf{x}^{(n)}$  is the displacement vector of element  $n$  which is measured relative to the local frame  $(x, y, z)$ , and  $k = 0$  for the head, and  $k = 1$  for the tail.

### 2.1 Geometrical Modelling

Consider a model micromachine, which has a head and a spiral tail, swimming in a viscous fluid by propagating distal spiral waves. Figure 1 illustrates two types of different spiral tails for this micromachine. In 1A, a spiral has been formed from twisting a rectangle about its lateral side, whereas in 1B the rectangle has been twisted about the principal centreline. Considering a micromachine with the tail of figure 1A will result in consuming more power as well as producing low propulsion velocity, since the path of this machine is not a straight line but a helix. The reason is that the tail is not symmetric with respect to its centreline for any value of the wave number  $N_w = L_t/\lambda$ ,  $\lambda$  being the wavelength, but the tail of the second model (B) is symmetric, hence it moves along a straight line. When the two micromachines are of the same size, the net forward velocity of the one of figure 1B is about 18% higher. Therefore, in this note, we focus on the geometrical optimisation of this type of micromachine. Here the thickness of tail is considered as zero, but a finite tail thickness can be accommodated without any change in the software. Different geometric parameters which have to be optimised, are shown in the same figure.

### 3 Optimisation procedure

Figure 1B shows the micromachine to be optimised dimensionally. The length of the rigid and inextensible tail of this machine,  $L_t$ , must remain constant. This length is also normalised to one. The centreline of the tail rotates relative to the head with an angular velocity of  $\omega$ . Therefore the spiral tail also rotates rigidly relative to the head with the same angular velocity  $\omega$ .

We start optimizing the wave number  $N_w$  along the tail. The numerical results reveal that the wave number has a slight effect on the angular velocity of the machine. However, the propulsion velocity  $U$  actually reaches a maximum at  $N_w = 1.5$  for each fixed set of values of  $L_t, b, a$  and  $L_h$ . Increasing the wave number will result in increasing the power, as Fig. 2 shows. The optimum value for the tail's wave number is exactly the same value derived by Phan-Thien et al. (1987) for an optimal microorganism with helical flagellum which requires a minimum power input.

To quantify the discretisation errors, different discretisation schemes were employed. For a machine with the dimensional geometry of the one shown in Fig. 2, values of

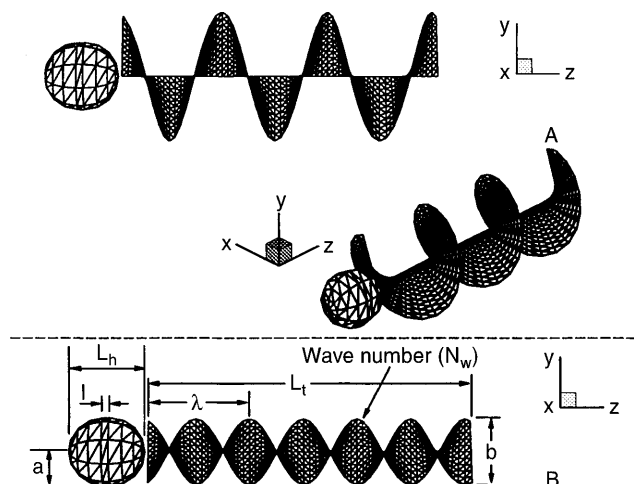


Fig. 1. Schematic diagram of two models of micromachines employing spiral waves along their tails

the velocity and the dissipated power converged to four significant digits when the number of elements exceeds  $10^3$  (to be exact, 1224). Errors due to discretisation have been shown in the same figure for two different boundary discretisation meshes of 864 and 1224 boundary elements. In the optimisation process carried out in this paper, when the size of the different parts of the body change, the number of the elements are increased appropriately to ensure an adequate convergence has been achieved.

The optimised wave number of the tail is then kept constant during the rest of this procedure.

As the radius of the head becomes exceedingly large compared with both  $L_t$  and  $b$  (on the left side of Fig. 3), we note that

$$\lim_{a \gg b} U = 0, \quad \lim_{a \gg b} \Omega = 0 .$$

Physically this means that the head of the micromachine is, in this limit, too large to be propelled by its tail.

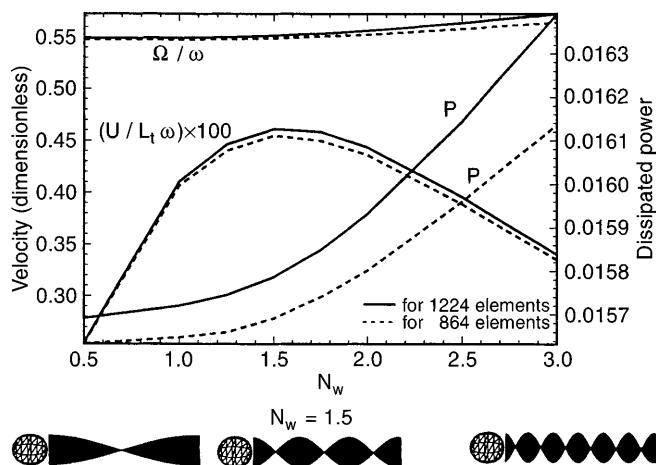


Fig. 2. The effect of the wave number  $N_w$  on the dimensionless velocities and dissipated power for  $L_t/a = 10, l/a = 0.2$  and  $L_t/b = 5$ . The optimal value is  $N_w = 1.5$ . Also the differences between the results for two boundary discretisation meshes are plotted

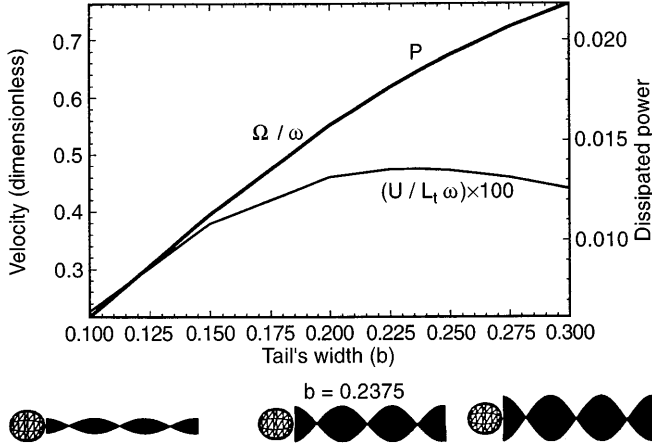


Fig. 3. The effect of tail's width,  $b$ , on the dimensionless velocities and power consumption for  $L_t/a = 10$ ,  $l/a = 0.2$  and  $N_w = 1.5$ . Optimum value is  $b/L_t = 0.2375$  is shown in the middle figure

To the other extremity, by increasing the tail's width, it is obvious from the graph that

$$\lim_{a \ll b} U = 0, \quad \lim_{a \ll b} \Omega = 1,$$

which means that the head will be rotating exactly with the same angular velocity of the tail but in the opposite direction.

These results are in agreement with Chwang and Wu's conclusions (1971) on the motion of microorganism with helical tail. They introduced the phase velocity  $c$

$$c = \omega/K,$$

where  $K$  was taken as  $2\pi/\lambda$ . They normalised the propulsive velocity with respect to this phase velocity and derived the optimum values for radius of the head and the tail. For our case, length scales and time are normalised with respect to the length of the tail  $L_t$  and  $\omega$ , respectively, we have

$$U/c = 2\pi U/\lambda = 2\pi N_w U.$$

Holding the wave number and also the width of the tail fixed, we found that the velocity of the machine increases with longer head (Fig. 4). Numerical results show that, when the head's length is 4.8 times of head's radius ( $L_h/a = 4.8$  or  $l/a = 2.8$ ), the velocity attains a maximum value. For large value of the head's length, the angular velocity of the head approaches to zero.

We next check the effect of changing both the head's radius and its length (Fig. 5), but keeping the ratio of the head's length to its radius,  $L_h/a$ , fixed at 4.8. We found that the optimal value for the ratio of the head's length to the tail's length or  $L_h/L_t$  is about 0.5334.

When the head of a micromachine becomes small ( $a \rightarrow 0$ ), it is clear from figure 5 (right hand side) that the forward propulsion velocity will also be small, and the induced angular velocity  $\Omega$  becomes nearly equal to the circular frequency,  $\omega = Kc$ , of the spiral wave. Thus the apparent angular velocity (viewed from a fixed point somewhere in the fluid far from machine), or  $\omega_{app} = \Omega - \omega$  is practically zero. Therefore, to an observer in the fixed frame of reference, the tail appears 'motionless', thus indicating that all motion of this class tend to

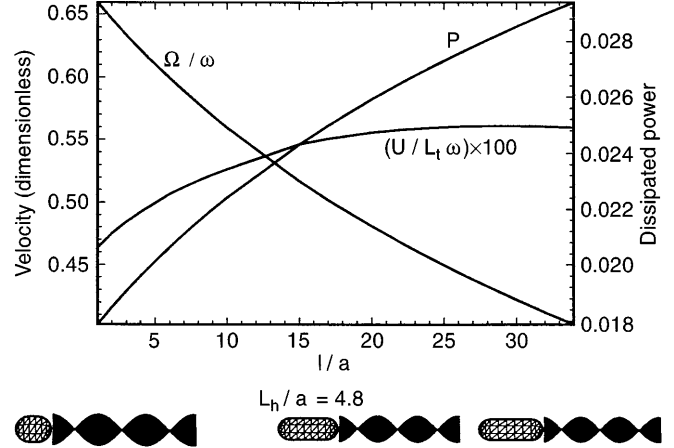


Fig. 4. The effect of the head's length,  $L_h$ , on the dimensionless velocities and dissipated power for  $L_t/a = 10$ ,  $N_w = 1.5$  and  $b/L_t = 0.2375$ . The velocity is maximised at  $L_h/a = 4.8$

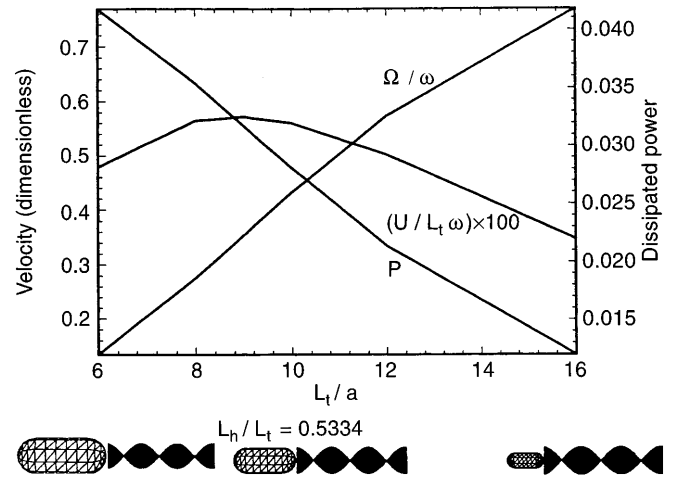


Fig. 5. Non-dimensional velocities and power consumption for different sizes of the head,  $N_w = 1.5$ ,  $b/L_t = 0.2375$ ,  $L_h/a = 4.8$ . Optimal value of  $L_h/L_t = .5334$  is obtained

cease and the machine becomes unable to propel itself by means of spiral wave. This conclusion agrees exactly with Chwang and Wu's results (1971). Before they proved this fact, Holwill and Burge (1963) and Holwill (1966) claimed that when the radius of the head approaches zero, the forward propulsion velocity will approach to a constant value, which is not correct. The physical interpretation of this result is now clear, because a micromachine, which has no head to resist the rotation given rise by the viscous torque due to its tail wave motion, simply cannot manifest spiral waves (or helical waves for the microorganism case).

The last part of this process is optimising the radius of the head which in fact has little effect on the translational velocity. Figure 6 shows that making the radius of the head bigger will result in an increase in the power consumption. The larger the radius of the head is, the smaller its angular velocity will be. From this, we can calculate the aspect ratio of the head which is about 0.47, in agreement with Bourrot's conclusion (1974) that the optimum body shape for

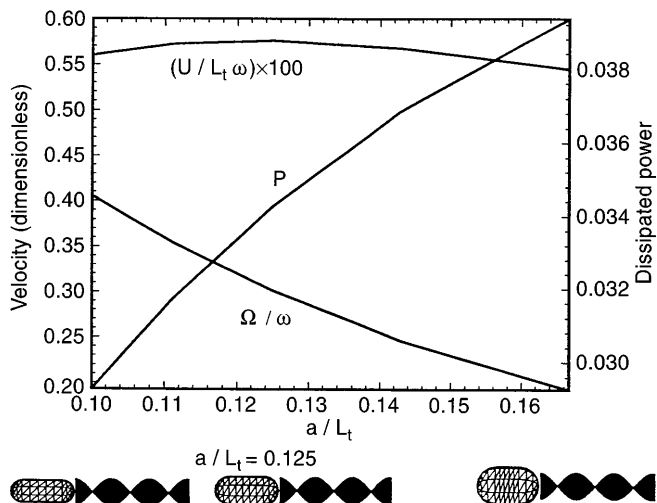


Fig. 6. Effects of the head diameter;  $N_w = 1.5$ ,  $b/L_t = .2375$  and  $L_h/L_t = .5334$ . The optimum value is  $a/L_t = .125$

head is nearly a prolate spheroid of aspect ratio about 0.5. For this special case, the result obtained here agrees well with the conclusions of Phan-Thien et al. (1987): the optimum ellipsoidal head (cell body) has an aspect ratios of 0.7 and 0.3.

#### 4

##### Conclusions

The problem of designing an efficiently swimming micromachine was addressed here. The mechanical model of this micromachine consisted of a capsule-shape head and rigid spiral shape tail which rotates relative to the head. Using the Boundary Element Method to calculate the velocity and traction on the boundary elements of this machine, the propulsion and angular velocity of the machine and the power consumption were obtained. In order to have the maximum net forward velocity, the optimal values or proportion of the head and the tail for this micromachine are as follows

$$N_w = 1.5, \quad b/L_t = 0.2375, \quad l/a = 2.2667, \\ L_h/L_t = 0.5334, \quad a/L_t = 0.125 .$$

This means that the optimum head has an aspect ratio of about 0.47; the tail has a length of about 8 times the radius of the head, about 4.21 times of its width and 1.5 wavelengths. The key result is that, for a given volume, the head should have minimum resistance to axisymmetric translation, while its moment of rotational inertia should be maximised.

The maximum non-dimensional translational velocity or  $U/L_t \omega$  was found to be  $0.58 \times 10^{-2}$  and therefore the forward propulsion velocity taking the phase velocity into account is equal to

$$U/c = .055 .$$

This value is close to the propulsion velocity of a micro-organism with optimum proportion which consumes the minimum power to propel itself in a viscous fluid (see Phan-Thien et al., 1987).

In conclusion, a micromachine with a spiral tail can swim in a viscous fluid as nearly as efficient as a micro-organism with helical tail and of the same size.

##### References

- Banerjee, P. K.; Butterfield, R. (1981): Boundary Element Methods in Engineering Science. McGraw-Hill, 138-167
- Bourot, J. M. (1974): On the computation of the optimum profile in Stokes flow. J. Fluid Mech. 65, 513-515
- Brebbia, C. A.; Telles, J. C. F.; Wrobel, L. C. (1984): Boundary Element Techniques: Theory and Application in Engineering. Springer-Verlag, Berlin 177-236
- Chwang, A. T.; Wu, T. Y. (1971): A note on the helical movement of micro-organisms. Proc. Roy. Soc. Lond. B 178, 327-346
- Chwang, A. T.; Wu, T. Y.; Winet, H. (1972): Locomotion of Spirilla. Bio. J. 12, 1549-1561
- French, P. J. (1996): Development of surface micromachining techniques compatible with on-chip electronics. J. Micromech. Microeng. 6 (2), 197-211
- Gray, J.; Hancock, G. J. (1955): The propulsion of sea-urchin spermatozoa, J. Exp. Biol. 32, 802-814
- Hancock, G. J. (1953): The self-propulsion of microscopic organisms through liquids. Proc. Roy. Soc. Lond. A 217, 96-121
- Holwill, M. E. J.; Burge, R. E. (1963): A hydrodynamic study of the motility of the flagellated bacteria. Archs. Biochem. Biophys. 101, 249-260
- Holwill, M. E. J. (1966): The motion of Euglena viridis; The role of flagella. J. Exp. Biol. 44, 578-588
- Keller, J. B.; Rubinow, S. I. (1976): Swimming of flagellated microorganisms, Bio. J. 16, 151-170
- Lighthill, M. J. (1976): Flagellar Hydrodynamics: the John Von Neumann Lecture 1975. SIAM Rev. 18, 161-229
- Nasser, S.; Phan-Thien, N. (1996): On the path and efficiency of two micromachines with rigid tails. Comp. Mech. 18 (3), 192-199
- Phan-Thien, N.; Tran-Cong, T.; Ramia, M. (1987): A boundary element analysis of flagellar propulsion. J. Fluid Mech. 184, 533-549
- Taylor, G. I. (1951): Analysis of the swimming of microscopic organism. Proc. Roy. Soc. Lond. A 209, 447-462
- Taylor, G. I. (1952): The action of waving cylindrical tails in propelling microscopic organism. Proc. Roy. Soc. Lond. A 211, 225-239